OncoTargets and Therapy

Dovepress
open access to scientific and medical research

Open Access Full Text Article

ORIGINAL RESEARCH

# TIM-3 Participates in the Invasion and Metastasis of Nasopharyngeal Carcinoma via SMAD7/SMAD2/SNAIL1 Axis-Mediated Epithelial-Mesenchymal Transition

This article was published in the following Dove Press journal:
*OncoTargets and Therapy*

Yangyang Xiao[1,*]
Jilin Qing[2,*]
Baoxuan Li[3]
Liuyan Chen[1]
Shengzhou Nong[1]
Wenhui Yang[1]
Xiaogang Tang[4]
Zhizhong Chen[1]

[1]Department of Clinical Laboratory, People's Hospital of Guangxi Zhuang Autonomous Region, Nanning, Guangxi 530021, People's Republic of China; [2]Center for Reproductive Medicine and Genetics, People's Hospital of Guangxi Zhuang Autonomous Region, Nanning, Guangxi 530021, People's Republic of China; [3]Department of Ophthalmology, Binzhou Medical University Hospital, Binzhou, Shandong 256603, People's Republic of China; [4]Department of Intensive Care Unit, People's Hospital of Guangxi Zhuang Autonomous Region, Nanning, Guangxi 530021, People's Republic of China

*These authors contributed equally to this work

**Background:** T-cell immunoglobulin and mucin domain-containing molecule-3 (TIM-3) was originally found to negatively regulate immune response and mediate immune escape in tumors. Subsequently, an increasing body of evidence has shown that TIM-3 exerts positive functions in the development and progression of several tumors. However, the role of TIM-3 in nasopharyngeal carcinoma (NPC) remains unknown.

**Methods:** Data from the Cancer Genome Atlas-head and neck squamous cell carcinoma and immunohistochemistry were analyzed to compare the expression of TIM-3 in NPC and non-cancerous nasopharyngitis tissues. Cell proliferation was evaluated using the Cell counting kit-8 in vitro and xenograft experiment in nude mice in vivo. Flow cytometry was used to evaluate the cell cycle. The migration and invasion of NPC cells were assessed through wound healing and Transwell assays. In addition, Western blotting was used to analyze the expression of specific proteins.

**Results:** Higher expression of TIM-3 was detected in NPC tissues than normal nasopharyngeal tissues and positively correlated with the clinical stage and T classification; however, it was not correlated with gender, age, and N classification. Furthermore, overexpression of TIM-3 using lentiviral vectors increased the malignancy of 6-10B and CNE-2 cell lines that lowly express TIM-3, by promoting cell proliferation, migration, and invasion in vitro and in vivo. In addition, overexpression of TIM-3 was associated with upregulation of matrix metalloproteinase 9 (MMP9) and MMP2, and led to epithelial-mesenchymal transition (EMT) by increasing the levels of mesenchymal markers (ie, N-cadherin, Vimentin) and decreasing those of the epithelial marker E-cadherin. Further study showed that SMAD7 was downregulated in the TIM-3 overexpression group. Relatively, phosphorylated SMAD2 and downstream molecule SNAIL1 were also upregulated in this group.

**Conclusion:** TIM-3 exerts a tumor-promoting function in NPC by mediating changes in the SMAD7/SMAD2/SNAIL1 axis. These findings provide a new idea for the study of invasion, metastasis, and treatment of NPC.

**Keywords:** nasopharyngeal carcinoma, T-cell immunoglobulin and mucin-domain containing molecule-3, invasion, metastasis, epithelial-mesenchymal transition

Correspondence: Zhizhong Chen
Department of Clinical Laboratory, People's Hospital of Guangxi Zhuang Autonomous Region, 6 Taoyuan Road, Nanning, Guangxi 530021, People's Republic of China
Tel +86 771 2186126
Email tjchenzz@126.com

## Introduction

Nasopharyngeal carcinoma (NPC) is an epithelial carcinoma arising from the nasopharyngeal mucosal lining. Its occurrence exhibits obvious geographical differences and >70% of new cases are reported in East and Southeast Asia. A combination of genetic, ethnic, and environmental factors may affect the pathogenesis of NPC.[1,2] The

submit your manuscript | www.dovepress.com
DovePress
http://doi.org/10.2147/OTT.S237222

definitive diagnosis of NPC is reached through endoscopic-guided biopsy of the primary tumor. Given the deep location and complex adjacency of the nasopharynx, it is difficult to perform radical surgical resection. NPC is highly sensitive to ionizing radiation, and radiotherapy is the mainstay treatment modality. Concurrent chemotherapy is always recommended for advanced-stage NPC.[3] A recent study reported that induction chemotherapy plus concurrent chemoradiotherapy shows an advantage in improving patient survival in the late stage of NPC.[4] With the development of therapeutic technology, the incidence and mortality rate linked to NPC have gradually declined over the past decades. Nevertheless, >20% of patients experience distant metastasis after treatment, resulting in a poor prognosis.[1]

T-cell immunoglobulin and mucin domain-containing molecule-3 (TIM-3) is a type-I glycoprotein distributed on the cell surface. It was originally identified as a molecule expressed on CD4+ T helper type 1 (Th1) cells, but not Th2 cells.[5,6] When combined with the ligand galectin 9, TIM-3 induces death of Th1 cells.[7] Subsequent research studies revealed that TIM-3 is expressed on natural killer cells, monocytes, and dendritic cells, performing different functions.[8–11] In view of the role of TIM-3 in immune regulation, TIM-3 is an immune checkpoint. With the research and development of tumor immunotherapy, TIM-3 has gained prominence as a potential candidate for cancer immunotherapy.[12] Accumulating evidence suggests that TIM-3 expression is not restricted to immune cells, and can be expressed on cancer cells, such as lung cancer,[13] cervical cancer,[14] hepatocellular carcinoma,[15] and prostate cancer.[16] However, the function of TIM-3 on different tumors is controversial.

Currently, studies investigating NPC and TIM-3 are limited to immunological changes in the tumor microenvironment.[17,18] However, the intrinsic expression of TIM-3 in NPC cells, the roles that TIM-3 plays in the progression and metastasis of NPC, and the exact mechanisms of TIM-3 involved in the development of NPC have not been elucidated. In preliminary experiments, we found that TIM-3 was differentially expressed in NPC cell lines with different metastatic abilities. We hypothesized that TIM-3 may be directly involved in the invasion and metastasis of NPC, and related to the occurrence and development of NPC. To confirm this hypothesis, we examined the expression of TIM-3 in NPC tissues and cell lines, and subsequently demonstrated the effects of TIM-3 on the malignant biological behavior of NPC and its possible mechanisms through in vivo and in vitro experiments.

# Materials and Methods

## Relative mRNA Expression of TIM-3 in the Cancer Genome Atlas-Head and Neck Squamous Cell Carcinoma (TCGA-HNSC)

The data for mRNA analysis were derived from TCGA[19] and aggregated via UALCAN as previously described.[20] NPC is one of the most common HNSC and shares many similarities with other head and neck tumors. Therefore, we extracted data from the TCGA-HNSC for analysis. In the cohort, TIM-3 RNA-seq data were collected from 519 patients with primary HNSC and 44 normal controls. The results were converted to transcript per million (TPM).

## Clinical Specimens

Nasopharyngeal biopsy specimens were obtained from 60 patients at the People's Hospital of Guangxi Zhuang Autonomous Region from 2016 to 2018. Patients had not received preoperative radiotherapy, chemotherapy, or biological therapy. The 60 patients included 48 NPC cases (31 men and 17 women) and 12 non-cancerous nasopharyngitis (NPG) cases (10 men and two women). Of all 48 cases of NPC, 33 had lymph node metastasis and the metastasis rate reached 68.75%. Clinical data of the patients with NPC were reviewed based on the pathological Tumor-Node-Metastasis staging system (American Joint Committee on Cancer/Union for International Cancer Control, 8th edition). Patients with NPC were first diagnosed at a median age of 47 years (range: 16–71 years). Following histological examination, all patients with NPC were diagnosed with non-keratinizing undifferentiated carcinoma. Research protocols were reviewed and approved by the Ethics Committees/Institutional Review Boards of the People's Hospital of Guangxi Zhuang Autonomous Region. All patients whose tissues were used in this study provided written informed consent. This study was conducted in accordance with the tenets of the Declaration of Helsinki.

## Immunochemical Staining

Three-step immunochemistry assay was performed using a Histostain-Streptavidin-Peroxidase Kit (Bioss, Beijing, China). Briefly, formalin-fixed and paraffin-embedded tissues (4 μm) were deparaffinized in xylene 20 min and rehydrated in gradient concentration alcohol (1 min per concentration). Subsequently, heat-induced antigen retrieval

was conducted in ethylenediaminetetraacetic acid buffer (pH 9.0) for 3 min in a pressure cooker. Endogenous peroxidase was blocked via incubation in 3% hydrogen peroxide for 20 min. Goat serum (10%) was used for blocking at room temperature for 20 min to avoid non-specific staining, followed by incubation of the section overnight at 4°C with a rabbit anti-human TIM-3 polyclonal antibody (1:500 dilution; Abcam, Cambridge, UK). Subsequently, sections were incubated with biotinylated goat anti-rabbit secondary antibody and horseradish peroxidase-labeled streptavidin for 20 min at room temperature. Diaminobenzidine was added to develop color and hematoxylin was used to stain cell nucleus. The scoring system used has been previously described.[21] Briefly, the staining intensity of TIM-3 was scored using a 0–3 scale (0, no staining; 1, weak staining; 2, moderate staining; 3, strong staining). Scores 0–1 and 2–3 were considered low and high, respectively.

## Reverse Transcription and Real-Time Quantitative Polymerase Chain Reaction (PCR)

Total RNA was isolated from cultured cell lines using RNAiso Plus (Takara, Dalian, China) according to the instructions provided by the manufacturer. First-strand cDNA was synthesized using the PrimeScript™ RT reagent Kit (Takara) according to the product manual. Subsequently, real-time quantitative PCR was performed on an ABI 7500 Real-Time PCR System (Thermo Fisher Scientific, Waltham, MA, USA) using a TB Green Premix Ex Taq™ II Kit (Takara). Briefly, the quantitative PCR conditions included a pre-denaturation step at 95°C for 30 s, followed by 40 cycles at 95°C for 5 s and 60°C for 34 s. A dissociation curve was used to determine the specificity of the reaction. The primer sequences, synthesized by Invitrogen (Carlsbad, CA, USA), were as follows: TIM-3, forward 5′-CAGATACTGGCTAAATGGGGAT-3′ and reverse 5′-ACCTTGGCTGGTTTGATGAC-3′; β-actin was used as the internal control, forward 5′-TGAC GTGGACATCCGCAAAG-3′, and reverse 5′-CTGGAA GGTGGACAGCGAGG-3′. The relative expression levels of TIM-3 were calculated using the $2^{-\Delta\Delta CT}$ method.[22] Each experiment was performed in triplicate.

## Cell Lines and Culture

NPC cell lines (CNE-2 and HK-1) were preserved in the Research Center of Medical Sciences, People's Hospital of Guangxi Zhuang Autonomous Region. Cell lines 5-8F and 6-10B were kindly provided by Professor Musheng Zeng (State Key Laboratory of Oncology in South China, Sun Yat-Sen University Cancer Center, Guangzhou, China). Both 5-8F and 6-10B cells were isolated from the SUNE-1 cell line; 6-10B was non-metastatic, whereas 5-8F was highly metastatic.[23] CNE-2, a low metastatic NPC cell line, was also used.[24] The cells were cultured in RPMI-1640 (Gibco, Carlsbad, CA, USA) supplemented with 10% fetal bovine serum (FBS; Gibco), 100 units/mL penicillin (Gibco), and 100 μg/mL streptomycin (Gibco). All cells were grown in a 5% $CO_2$ environment at 37°C. Use of all the cell lines was approved by the Ethics Committees/Institutional Review Boards of the People's Hospital of Guangxi Zhuang Autonomous Region.

## Lentivirus Transfection and Establishment of Stable Cell Lines

The LV5-TIM-3 homo and LV5-negative control (NC) lentiviral vectors were purchased from GenePharma Co. (Suzhou, China). Cell transfection was performed according to the protocol provided by the manufacturer; the multiplicity of infection used in the 6-10B and CNE-2 cell lines was 100. Puromycin, 3 μg/mL (6-10B) and 2 μg/mL (CNE-2) (Leagene, Beijing, China), was used for 1 week to select stably transfected cells until the transfection efficiency reached >90%.

## Cell Proliferation

Cell counting kit-8 (CCK-8) and plate colony formation assays were performed to evaluate the ability of cell proliferation according to instructions provided by the manufacturer. For the CCK-8 assay, 1000 (6-10B) or 2000 (CNE-2) cells in 100 μL 10% FBS medium were seeded into 96-well plates and cultured for 24, 48, 72, 96, and 120 h. The CCK-8 reagent (Meilun, Dalian, China) (10 μL) and 10% FBS-containing medium (90 μL) were replaced at each time point. After incubation at room temperature for 3 h, the absorbance was measured at 450 nm using a Microplate Reader (BioTek, Winooski, VT, USA). For the colony formation assay, 500 cells were seeded into six-well plates and cultured for 10 days (6-10B) or 15 days (CNE-2). The colonies were washed with phosphate-buffered saline, fixed with methanol for 30 min, and stained with 0.1% crystal violet for 20 min. Colonies containing >50 cells were counted. All experiments were performed in triplicate.

## Cell Cycle Analysis Using Flow Cytometry

The transfected and selected 6-10B or CNE-2 cells were collected when they reached the logarithmic growth phase. The cells were fixed with 70% alcohol overnight at 4°C, stained with propidium iodide/RNase Staining Buffer (BD Biosciences, San Diego, CA, USA), and assayed using a FACScan flow cytometer (BD FACSCanto™ II; BD Biosciences).

## Wound Healing Assay

The stably transfected 6-10B and CNE-2 cells were seeded on six-well plates at a density of $10^6$ cells per well. When the cells reached 90% confluence, three parallel scratches were performed using a 200-μL pipette tip. The cells were washed thrice with 1×phosphate-buffered saline to remove floating cells. Respective images were captured at 0, 12, 24 h (6-10B) or 0, 24, 48 h (CNE-2) using a microscope (original magnification: ×100; Olympus). The width of the original scratch and that measured after cell migration in five randomly fields was used for comparison at each time point.

## Migration and Invasion Assays

Cell migration and invasion assays were performed in 24-well Transwell cell culture chambers or Biocoat matrigel invasion chamber (Corning, Cambridge, MA, USA). Rehydration of the invasion chamber was performed prior to use according to the instructions provided by the manufacturer. A total of $3\times10^4$ cells in serum-free medium (150 μL) were seeded into the upper chamber and RPMI-1640 medium (600 μL) containing 15% FBS was added into the lower chamber. After culture for 20–24 h (migration assay) or 30–36 h (invasion assay), cells were fixed with methanol for 30 min and stained with 0.1% crystal violet for 20 min. Five random fields per well were observed under a microscope (original magnification: ×200; Olympus). Both experiments were performed in triplicate.

## Xenograft Experiment in Nude Mice

Twelve female BALB/c nude mice (age: 4–6 weeks) were purchased from Guangxi Medical University Animal Center (Nanning, China) and housed under specific-pathogen-free conditions. The mice were divided into NC group and TIM-3 randomly. A total of $2\times10^6$ transfected 6-10B cells in serum-free medium (200 μL) were subcutaneously injected into the right flank of each nude mouse. The tumor volumes were measured once every 3 days. All mice were euthanized when the tumor volume exceeded 1000 $mm^3$, and the volume and weight of tumor tissues were measured. The tumor volumes were calculated as follows: $(A\times B^2)/2$, in which A and B represent the largest and shortest diameter, respectively. All animal assays were approved by the Ethics Committees/Institutional Review Boards of People's Hospital of Guangxi Zhuang Autonomous Region. The experiments were conducted in accordance with $NC3R_S$ Arrive guidelines.

## Western Blotting

Total protein was isolated using radioimmunoprecipitation assay (RIPA) lysis buffer that contained a protease and phosphatase inhibitor cocktail (Solarbio, Beijing, China). The protein extracts were separated through SDS-PAGE and transferred onto polyvinylidene difluoride (PVDF) membranes ((Millipore, Billerica, MA, USA). The membranes were subsequently blocked in 5% defatted milk or bovine serum albumin (for phosphorylated protein), and incubated with rabbit anti-human antibodies overnight at 4°C. The primary antibodies used were anti-β-actin (1:1000; Bioss, Beijing, China), anti-TIM-3 (1:1000; Abcam), anti-SMAD7 (1:1000; Proteintech, Rosemont, IL, USA), anti-SNAIL1 (1:800; Proteintech), anti-E-cadherin (1:4000; Proteintech), anti-N-cadherin (1:4000; Proteintech), anti–Vimentin (1:4000; Proteintech), anti-MMP2 (1:1000; Proteintech), anti-MMP9 (1:1000; Proteintech), and anti-SMAD2 (1:1000; Cell Signaling Technology, Danvers, MA, USA), anti-phospho-SMAD2 (Ser 465/467, 1:1000; Cell Signaling Technology). The secondary antibody used was horseradish peroxidase-conjugated goat anti-rabbit antibody (1:10,000; Abcam). Proteins were visualized with an enhanced chemiluminescence (ECL) detection system (Meilun). Images were captured using the Odyssey Fc Imaging System (LI-COR Biosciences, Lincoln, NE, USA).

## Statistical Analysis

The statistical analysis was performed using the GraphPad Prism 5 (GraphPad Software, San Diego, CA, USA) and SPSS 22.0 (IBM Corp., Armonk, NY, USA) software. A $P<0.05$ denoted statistical significance. The relationship between the expression of TIM-3 and the clinical parameters of clinical samples was assessed using the chi-squared test. The remaining experiments were performed in triplicate, and the data are presented as the mean ± standard deviation. Two-tailed unpaired Student's *t*-test was used for comparisons between different groups.

# Results

## The Expression of TIM-3 Is Elevated in NPC Tissues

We first searched TCGA, and extracted and aggregated data to observe the expression levels of TIM-3 in HNSC. As shown in Figure 1A, the expression levels of TIM-3 mRNA in HNSC were significantly higher (approximately two-fold) than those of the control. Subsequently, immunohistochemistry was performed to detect the expression levels of TIM-3 protein in biopsy specimens of NPC or NPG, as mentioned above. It was obvious that TIM-3 protein was localized diffusely in the cellular membrane and cytoplasm of tumor cells (Figure 1B and C). In some NPG specimens, we also found strong expression of TIM-3 in tumor infiltrating cells, but not normal nasopharyngeal epithelial cells (Figure 1D). As shown in Table 1, positive staining for TIM-3 was present in 91.7% (44/48) and 58.3% (7/12) of NPC and NPG tissue sections, respectively. The protein expression of TIM-3 was significantly higher in NPC tissues than NPG tissues (P=0.015).

## TIM-3 Expression and Clinicopathological Characteristics

In addition, we investigated the association of TIM-3 expression with several clinicopathological characteristics (ie, gender, age, clinical classification, T classification, N classification). We found that TIM-3 expression was positively correlated with clinical classification and T classification (P=0.03 and 0.012, respectively). However, there were no significant differences observed between TIM-3 expression and age, gender, and N classification (Table 2). These results indicated that TIM-3 may contribute to the progression of NPC.

**Table 1** Expression of TIM-3 in NPC and NPG Tissues

| Patients Type | Cases | TIM-3 Expression | | *P*-value |
|---|---|---|---|---|
| | | Negative | Positive | |
| NPC | 48 | 4 | 44 | *0.015 |
| NPG | 12 | 5 | 7 | |

**Note:** *$P<0.05$.
**Abbreviations:** NPC, nasopharyngeal carcinoma; NPG, nasopharyngitis.

## Expression of TIM-3 in Human NPC Cell Lines and Lentiviral Transfection for the Overexpression of TIM-3

We next determined the mRNA and protein levels of TIM-3 in several human cell lines (ie, 6-10B, CNE-2, HK-1, 5-8F) through qRT-PCR and Western blotting to investigate its role and mechanism in NPC. The results showed that the mRNA (Figure 2A) and protein (Figure 2B) levels of TIM-3 in non-metastatic 6-10B and low-metastatic CNE-2 cell lines were clearly lower than those recorded in the other two cell lines. These results imply that TIM-3 is associated with the metastasis of NPC.

Furthermore, we overexpressed TIM-3 in 6-10B and CNE-2 cells using lentiviral vectors with full-length

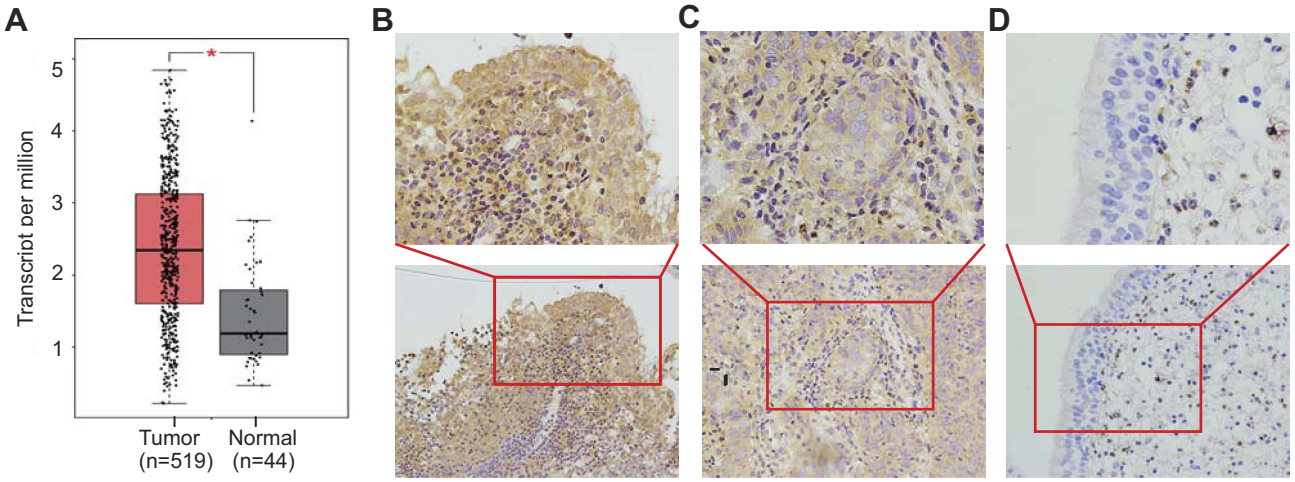


**Figure 1** Upregulation of TIM-3 in NPC tissues.
**Notes:** (**A**) TIM-3 mRNA expression levels in patients with HNSC in TCGA dataset cohorts. (**B**–**D**) Immunohistochemical staining of TIM-3 expression in NPC tissues. (**B**) Strong expression of TIM-3 protein in NPC tissues. (**C**) Moderate expression of TIM-3 protein in NPC tissues. (**D**) Negative expression of TIM-3 in NPC tissues, but strong staining in inflammatory cells. Lower panels, ×200 magnification; upper panels, ×400 magnification. *$P<0.05$.
**Abbreviations:** TIM-3, T-cell immunoglobulin and mucin domain-containing molecule-3; NPC, nasopharyngeal carcinoma.

**Table 2** Correlation of TIM-3 Expression and Clinicopathological Features of NPC Cases

| Items | TIM-3 (n) | | $X^2$ | *P*-value |
|---|---|---|---|---|
| | High Expression n=36 | Low Expression n=12 | | |
| Gender | | | | |
| Male | 23 | 4 | 0 | 1 |
| Female | 13 | 8 | | |
| Age (years) | | | | |
| ≥60 | 9 | 4 | 0.035 | 0.851 |
| <60 | 27 | 8 | | |
| Clinical classification | | | | |
| I–II | 6 | 8 | 8.605 | *0.03 |
| III–IV | 30 | 4 | | |
| T classification | | | | |
| T1-T2 | 13 | 10 | 6.261 | *0.012 |
| T3-T4 | 23 | 2 | | |
| N classification | | | | |
| N0-N1 | 22 | 9 | 0.273 | 0.601 |
| N2-N3 | 14 | 3 | | |

**Note:** *$P<0.05$.

TIM-3 (TIM-3 group). Transfection of cells with empty lentiviral vectors was also performed (NC group). After screening with puromycin, the mRNA (Figure 2C and E) and protein (Figure 2D and F) levels of TIM-3 in 6-10B and CNE-2 cells were obviously elevated. The NC and TIM-3 groups were used for subsequent experiments.

## Overexpression of TIM-3 Promotes Cell Proliferation Both in vitro and in vivo

CCK-8 and colony formation assays were first performed in vitro to observe changes in the proliferation ability of TIM-3-overexpressing cells. The results of the CCK-8 assay showed that the absorbance at 450 nm of the TIM-3 group was significantly higher in 6-10B (Figure 3A) and CNE-2 (Figure 3C) cells than that of the NC group after day 2. Meanwhile, these results were confirmed by the colony formation assays (Figure 3B and D). Subsequently, we performed cell cycle analysis using flow cytometry. Consistent with the CCK-8 and colony formation assays, the results showed a decreased percentage of cells in the G1 phase of the TIM-3 group in 6-10B cells compared with that noted in the NC group; the percentage of cells in the S phase was increased (Figure 3E). Similar results were obtained for the CNE-2 cells (Figure 3F).

Moreover, we established xenograft tumor models by injecting transfected 6-10B cells into nude mice to investigate whether TIM-3 exerted a similar growth-promoting effect in vivo. As shown in Figure 4A–C, the tumor volumes and weights were increased in the TIM-3 group versus the NC group. Thus, TIM-3 appears to act as a proliferation factor in the growth of NPC cells.

## Alteration of TIM-3 Expression Affects the Migration and Invasion Ability of NPC Cells in vitro

We performed wound healing, transwell migration, and invasion assays in transfected 6-10B and CNE-2 cells to examine whether TIM-3 influences the metastatic ability of NPC cells. The wound healing assay demonstrated that migration in the TIM-3 group was markedly more rapid than that observed in the NC groups in both 6-10B and CNE-2 cells (Figure 5A). In the Transwell migration assay, we observed that the number of cells which migrated through the membrane was markedly increased in the TIM-3 group of 6-10B and CNE-2 cells (Figure 5B). A more pronounced cell penetration rate was observed in the Transwell invasion assay (Figure 5C). The results showed that TIM-3 altered the ability of the cells to migrate and increased their ability to hydrolyze the matrix.

## Overexpression of TIM-3 Altered Metastasis-Related Molecules in NPC Cells

MMP2 and MMP9 are two classic molecules belonging to the matrix metalloproteinase family that promote metastasis by hydrolyzing the extracellular matrix.[25,26] We first examined whether their expression was altered in the TIM-3 overexpression group through Western blotting. As shown in Figure 6A, in 6-10B cells, the expression of MMP2 and MMP9 was markedly upregulated in the TIM-3 group versus the NC group. The result for MMP2 in CNE-2 cells was consistent with that observed for 6-10B cells. However, there was no statistically significant difference in the elevation of MMP-9 in CNE-2 cells (Figure 6B).

In addition, epithelial-mesenchymal transition (EMT) is an important manifestation of loss of adhesion and acquisition of metastatic potential in tumor cells.[27] We evaluated the expression of several EMT-related markers to confirm whether TIM-3 promotes the motility of NPC cells via EMT. In both 6-10B and CNE-2 cells, the levels of the epithelial marker E-cadherin were significantly lower in

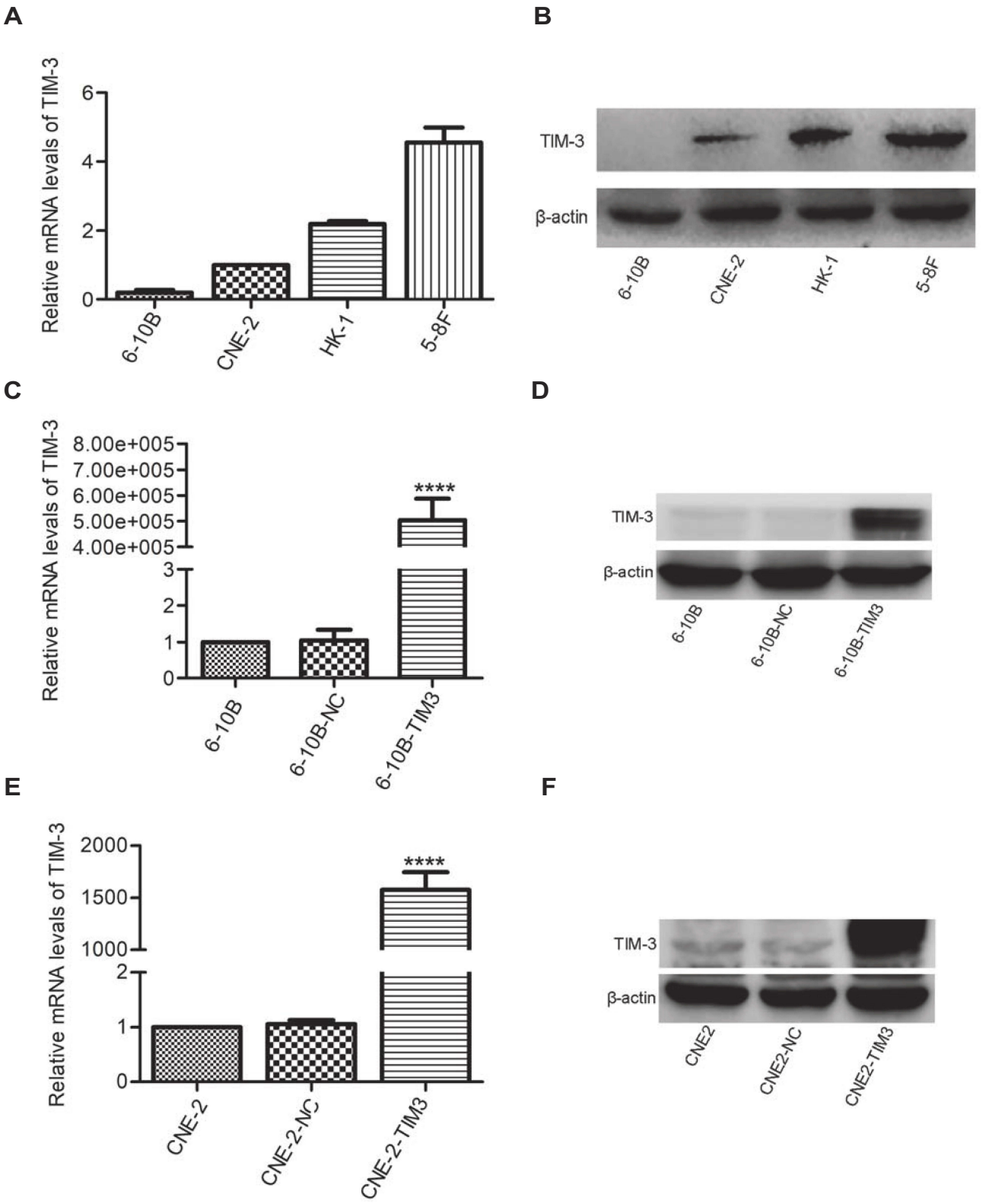


**Figure 2** Differences in the expression of TIM-3 in NPC cell lines and verification of the effect through overexpression of TIM-3.

**Notes:** (**A**) The expression of TIM-3 at the mRNA level in four NPC cell lines was analyzed using qRT-PCR. (**B**) The expression of TIM-3 at the protein level in NPC cell lines was analyzed through Western blotting. (**C, D**) The expression of TIM-3 was significantly elevated at both the mRNA (**C**) and protein (**D**) levels in 6-10B. (**E, F**) The expression of TIM-3 was significantly elevated at both the mRNA (**E**) and protein (**F**) levels in CNE-2. β-actin was used for normalization. Data shown as mean ± SD. ****$P$<0.0001 vs the NC group.

**Abbreviation:** NC, negative control.

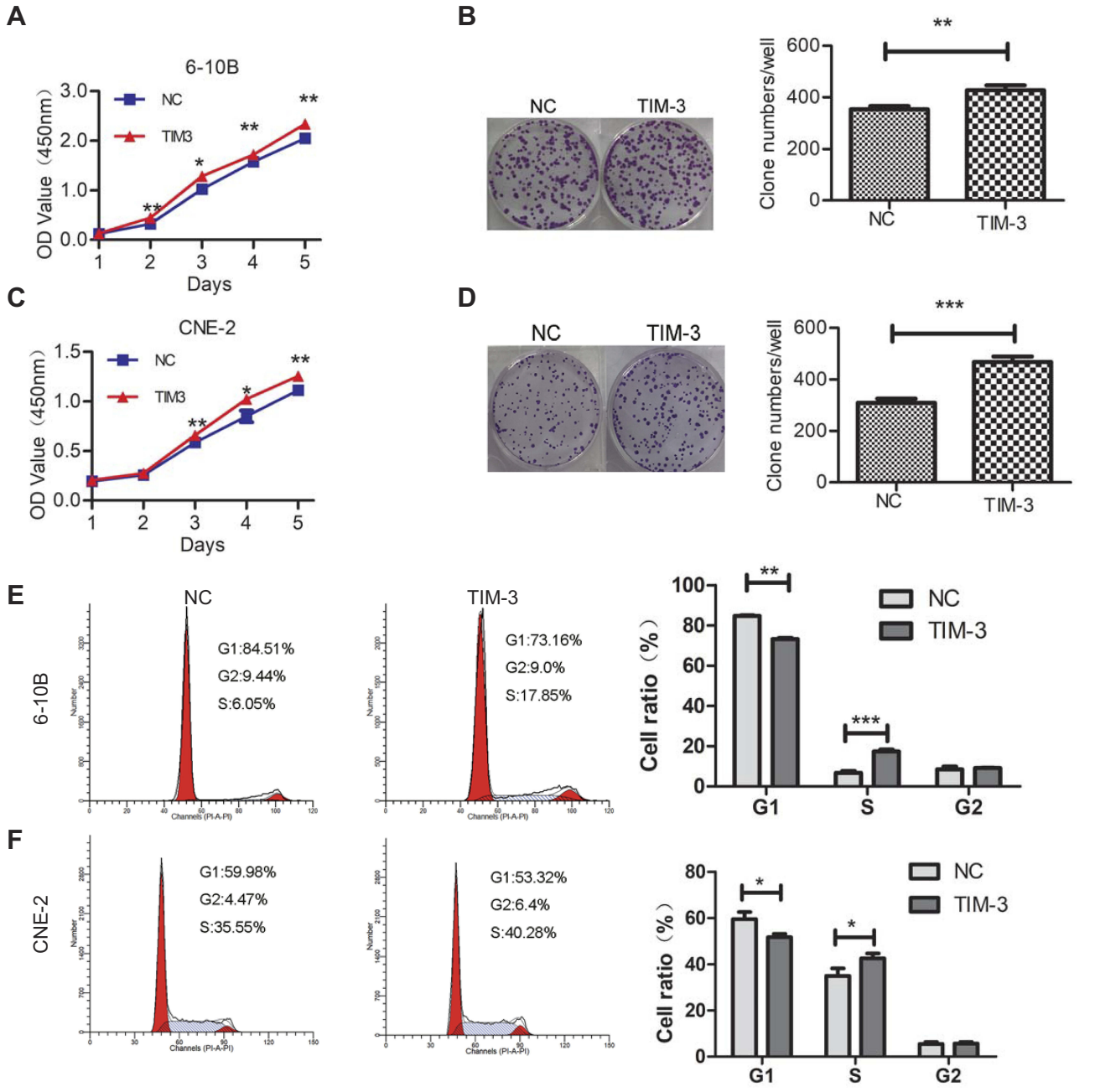


**Figure 3** Overexpression of TIM-3 promotes proliferation and alters the cell cycle in NPC cells.
**Notes:** (**A**–**D**) Proliferation of 6-10B (**A, B**) or CNE-2 (**C, D**) cells after overexpression of TIM-3. (**A**) CCK-8 assay in 6-10B cells. (**B**) Clone formation assay in 6-10B cells. (**C**) CCK-8 assay in CNE-2 cells. (**D**) Clone formation assay in CNE-2 cells. (**E**) Cell cycle analysis using flow cytometry in 6-10B cells. (**F**) Cell cycle analysis using flow cytometry in 6-10B cells. Data shown as mean ± SD. **P*<0.05, ***P*<0.01, ****P*<0.001 vs the NC group.

the TIM-3 group versus the NC group. However, an opposite result was noted for mesenchymal markers N-cadherin and Vimentin (Figure 6A and B). Therefore, the data showed that TIM-3 enhanced the metastasis of NPC cells by inducing EMT and promoting matrix hydrolysis.

## TIM-3 Promotes the Migration and Invasion of NPC Cells Through Alteration of the SMAD7/SMAD2/SNAIL1 Axis

The above results showed that the EMT process occurred in the TIM-3 overexpression group of NPC cell lines. It

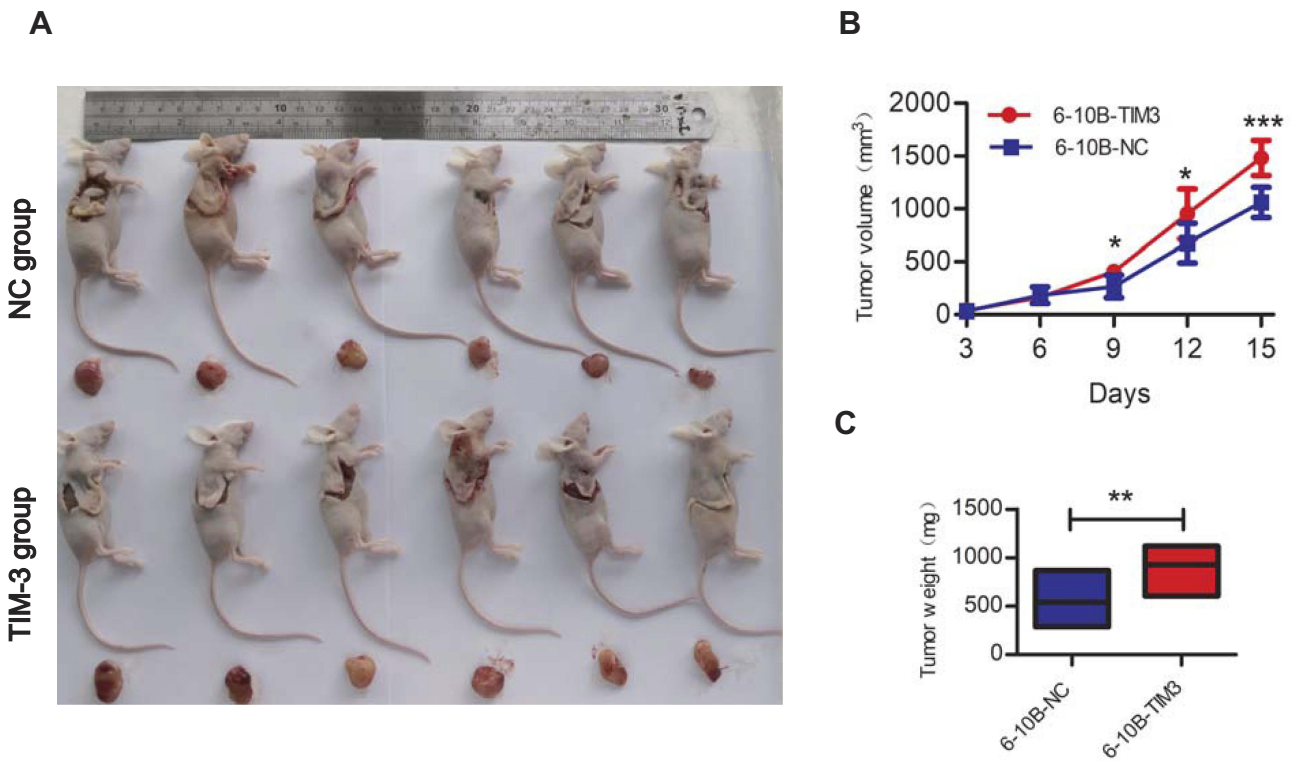


**Figure 4** Upregulation of TIM-3 accelerates tumor growth in vivo.
**Notes:** Transfected 6-10B cells were subcutaneously implanted. (**A**) Images of nude mice and tumors from both groups are shown. (**B**) The growth curve of tumor size. (**C**) Tumor weight at the end of the experiments. Data shown as mean ± SD. *$P$<0.05, **$P$<0.01, ***$P$<0.001.

has been reported that phosphorylation of SMAD2 leads to EMT in tumors; SMAD7 can reverse this process by inhibiting the phosphorylation of SMAD2.[28] We first evaluated the expression of SMAD7, SMAD2, and phosphorylated SMAD2 through Western blotting to examine the role of these molecules in TIM-3-overexpressing NPC cells. As shown in Figure 7A and B, overexpression of TIM-3 significantly increased the phosphorylation of SMAD2 and attenuated the expression of SMAD7 in both 6-10B and CNE-2 cells. SNAIL1, a downstream molecule inducing EMT in tumors, was subsequently examined. Consistently, the expression of SNAIL1 was significantly elevated in the TIM-3 overexpression group versus the NC group in both cell lines. Collectively, our results support the conclusion that overexpression of TIM-3 promoted EMT of NPC by mediating alterations in the SMAD7/SMAD2/SNAIL1 axis.

## Discussion

Immunosuppression of the tumor microenvironment is an important process of tumorigenesis and development. TIM-3 can be co-expressed with programmed cell death 1 (PD1) in tumor-infiltrating $CD8^+$ T lymphocytes to induce dysfunction of $CD8^+$ T lymphocytes in both solid and hematological tumors.[29,30] This concept carries great potential for targeting TIM-3 with or without PD1 to relieve immunosuppression of the tumor microenvironment, restoring the function of $CD8^+$ T cells in controlling tumor progression.[12,31] Studies have shown that the exosomes released by NPC cells contain galectin 9, which circulates in the tumor microenvironment and blood and binds to TIM-3 on the surface of Th1 cells, exerting an immunosuppressive effect on Th1 cells. Use of blocking anti-TIM-3 and anti-galectin 9 antibodies can prevent this effect.[32] These results suggest that TIM-3 may interact with its ligand to regulate T cell activation, indirectly participate in the invasion and metastasis of NPC, and be related to the occurrence and development of tumors.

It is been found that TIM-3 is also expressed in tumor cells and tissues of several cancers; however, its role in different tumors is controversial. The expression of TIM-3 is upregulated in various cancers, including non-small cell lung cancer, cervical cancer, and hepatocellular carcinoma.[13–15] Several recent studies showed that higher expression of TIM-3 is negatively correlated with the survival time of patients with cancer.[33,34] Knockdown of TIM-3

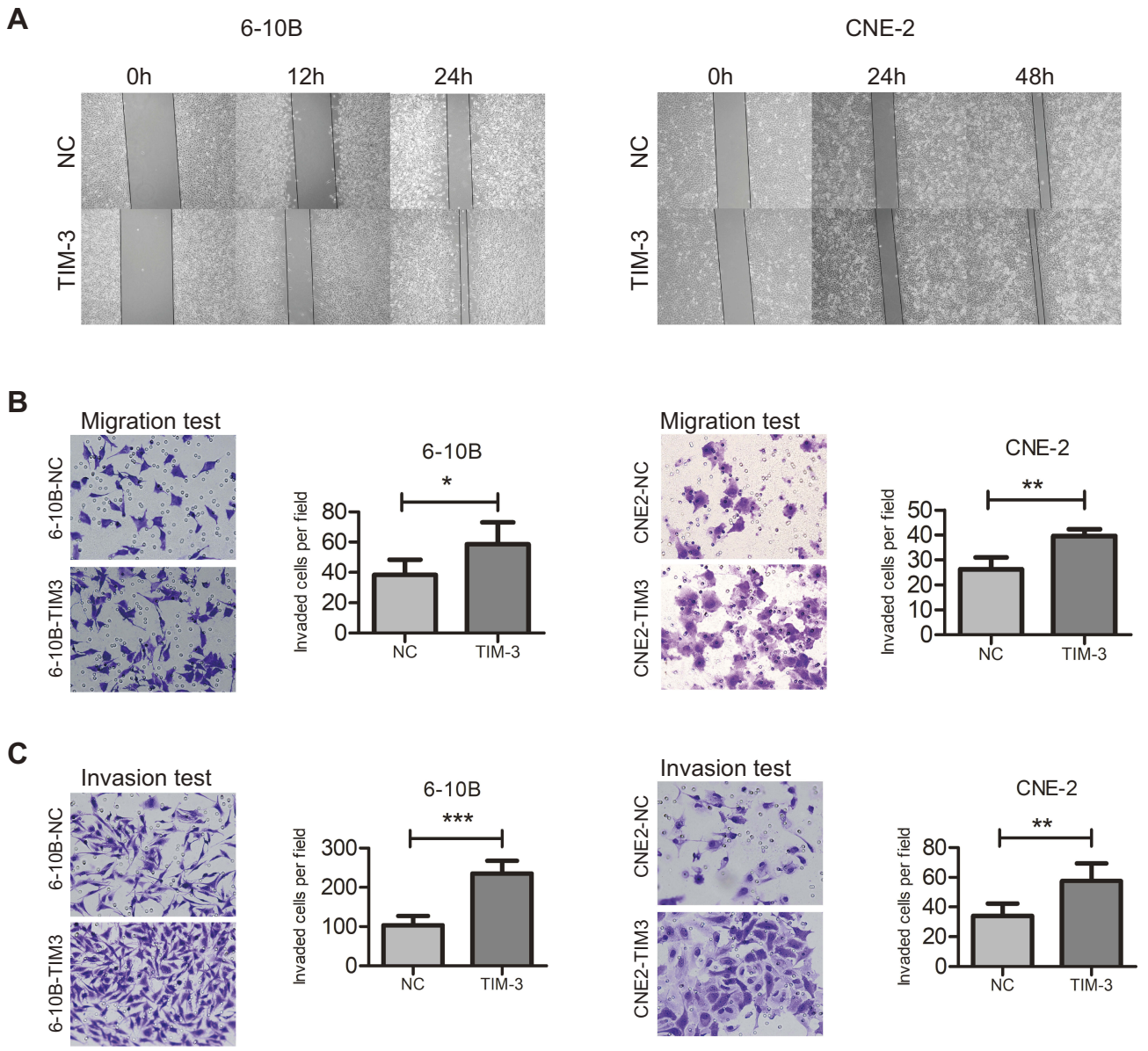


**Figure 5** Overexpression of TIM-3 promotes the migratory and invasive potential of NPC cells.
**Notes:** (**A**) Wound healing assay was performed to examine the migratory potential of 6-10B (left panel) and CNE-2 (right panel) cells at three timepoints, ×100 magnification. (**B**) Transwell migration test of 6-10B (left panel) and CNE-2 (right panel) cells, ×200 magnification. (**C**) Matrigel invasion test of 6-10B (left panel) and CNE-2 (right panel) cells, ×200 magnification. Data shown as mean ± SD. **P*<0.05, ***P*<0.01, ****P*<0.001.

inhibits proliferation, migration, and invasion in esophageal squamous cell carcinoma cell lines.[35] However, it was also found that TIM-3 expression is downregulated in prostate cancer, and low TIM-3 expression is associated with poor prognosis and metastasis.[16] Similar findings were reported in colon cancer.[36] However, the expression of TIM-3 in NPC cells and its effects on the progression and metastasis of NPC remain unknown. Recurrent and distant metastases are the main causes of death in patients with NPC. Hence, it is crucial to identify new targets for controlling the malignant metastasis of NPC. The present study systematically illustrated the possible functions of TIM-3, which may directly participate in the invasion and metastasis of NPC, and is related to the occurrence and development of NPC, as well as its potential as a therapeutic target for NPC.

We firstly searched TCGA database to explore the expression of TIM-3 in NPC tissues. The results showed that the mRNA levels of TIM-3 in HNSC tissues were approximately two-fold higher than those observed in normal tissues. NPC is one of the most common types of HNSC and shares many similarities with other head and neck tumors. Thus, we verified that the expression of TIM-3 protein in

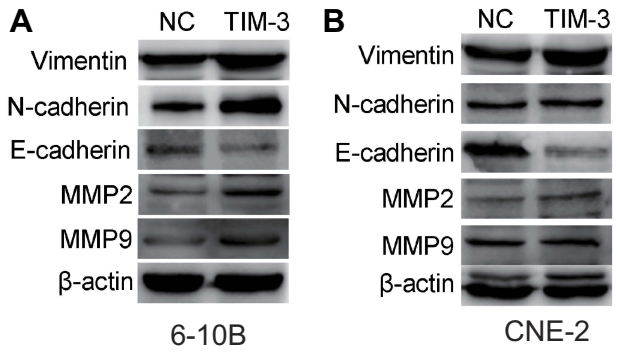


**Figure 6** Upregulation of TIM-3 alters the expression of metastasis-related molecules in 6-10B (**A**) and CNE-2 (**B**) cells through Western blotting.
**Note:** β-actin was used for normalization.

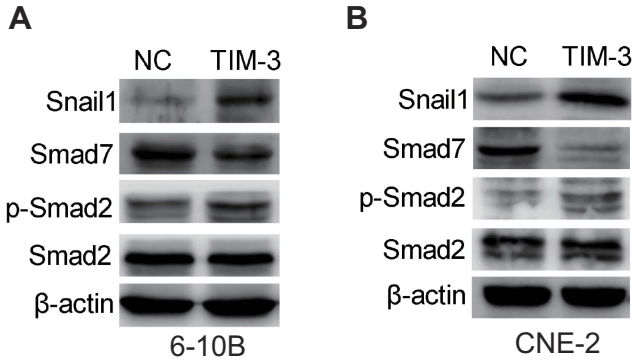


**Figure 7** Overexpression of TIM-3 alters the SMAD7/SMAD2/SNAIL1 axis.
**Notes:** Expression of SMAD7, SMAD2, p-SMAD2, SNAIL1 in 6-10B (**A**) and CNE-2 cells (**B**) was assessed through Western blotting.

NPC tissues was similar to that reported in HNSC using immunohistochemistry. It was demonstrated that TIM-3 expression was significantly higher in NPC tissues versus normal nasopharyngeal tissues. Moreover, this expression was positively correlated with the clinical stage, which is consistent with the results previously reported in liver, esophageal, and cervical cancers.[14,15,35] The expression levels of TIM-3 mRNA and protein in four NPC cell lines with different metastatic potentials were also detected. We found that TIM-3 was relatively hardly expressed in non-metastatic 6-10B cells, lowly expressed on low-metastatic CNE-2 cells, and highly expressed in high-metastatic 5-8F cells. Based on the above results, we suspected that TIM-3 may play a role in promoting metastasis in NPC.

Malignant proliferation is one of the main features of tumors.[37] We examined the changes in growing capacity, clone formation ability in vitro, and tumor formation ability in vivo of TIM-3-overexpressing NPC cells to observe whether TIM-3 exerted an effect on proliferation. As shown in the results, overexpression of TIM-3 significantly enhanced cell proliferation and clone formation ability in vitro, as well as tumor growth in nude mice in vivo. Subsequently, by performing cell cycle distribution analysis, we found that overexpression of TIM-3 resulted in G1 to S phase transition. Considering that dysregulation of G1 and G1/S checkpoint responses is an important cause of malignant proliferation of cancers, it is reasonable to suggest that overexpression of TIM-3 promotes growth of NPC cells by altering cell cycle distribution.[38]

Increased ability of cells to invade and migrate is another feature of malignant changes in cancer.[37] Through wound healing and transwell migration experiments, we found that overexpression of TIM-3 significantly increased the mobility of NPC cells. In addition, through Transwell invasion experiments, we found that overexpression of TIM-3 increased the ability of NPC cells to penetrate the matrix more effectively. This finding suggested that upregulation of TIM-3 increased the ability of cells to hydrolyze the extracellular matrix. Previous research showed that MMP2 and MMP9 can hydrolyze the extracellular matrix and promote invasion of tumor cells.[39] Our results demonstrated that the expression of MMP2 was significantly enhanced in 6-10B and CNE-2 cells following the overexpression of TIM-3. The expression of MMP9 was obviously enhanced in 6-10B cells. In contrast, there was no significant change in CNE-2 cells. This variation may be attributable to the differential invasiveness and metastatic abilities of the cell lines, as well as differences in the expression of MMP9 itself. In short, our results showed that TIM-3 can increased the ability of cells to hydrolyze the extracellular matrix and promote the invasion of NPC cells by elevating the levels of MMP2 and MMP9.

EMT is responsible for the increased ability of tumor cells to leave the primary tumor site, invade surrounding tissues, and establish distant metastases.[40] N-cadherin and Vimentin are two important markers of mesenchymal cells, and their expression increased; in contrast, there was a decrease in the expression of E-cadherin, an important marker of epithelial cells that usually appears in the EMT process.[27] The results showed that the expression of N-cadherin and Vimentin was significantly increased in the TIM-3 group, whereas that of E-cadherin was significantly decreased. Taken together,

our results showed that overexpression of TIM-3 induced EMT in NPC cells.

The SMAD proteins exhibit critical functions in metastasis formation and EMT.[41] Our results showed that the expression of SMAD7 was significantly reduced. There was no significant change in total SMAD2, whereas the expression of p-SMAD2 was significantly elevated. At the same time, the expression of SNAIL1 was significantly enhanced. SMAD7 is an inhibitory molecule that attenuates the phosphorylation of SMAD2.[42] Several studies have shown that enhanced SMAD7 expression inhibits metastasis and repression of SMAD7 induces EMT in human breast cancer.[43,44] EMT is driven by an interactive network of transcriptional repressors including SNAIL1; the upregulation of SNAIL1 can induce EMT.[45] The activation of SMAD2 proteins directly stimulates the expression of SNAIL1.[28] SNAIL1 is unique, because it can combine with the E-box sequences of the E-cadherin promoter to suppress the expression of E-cadherin, thus leading to the enhancement of EMT.[46] Based on the above results, our study suggests that TIM-3 alters the SMAD7/SMAD2/SNAIL1 axis, which leads to EMT and plays an important role in the invasion and metastasis of NPC (Figure 8).

In conclusion, the present findings suggest that TIM-3 acts as a cancer-promoting factor in NPC and can be used as a candidate biomarker for the clinical progression of NPC. Further, our study confirms that TIM-3 participates in NPC invasion and metastasis via SMAD7/SMAD2/SNAIL1 axis-mediated EMT. Our research will provide a new perspective for the pathogenesis and treatment of NPC.

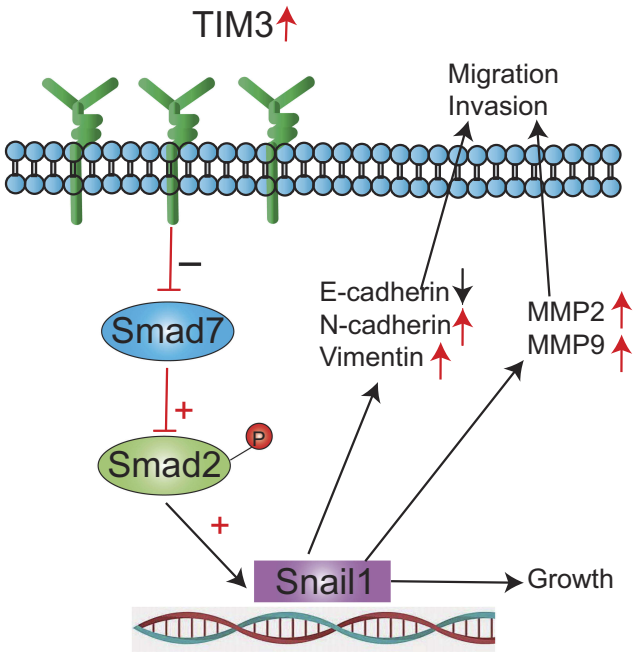


**Figure 8** Molecular mechanism of TIM-3-mediated invasion and migration of NPC.
**Note:** TIM-3 participates in NPC invasion and metastasis via SMAD7/SMAD2/SNAIL1 axis-mediated EMT.

## Ethics Approval and Consent to Participate

This study was approved by the Ethics Committees/Institutional Review Boards of People's Hospital of Guangxi Zhuang Autonomous Region. All patients whose tissues were used in this study provided written informed consent.

## Data Sharing Statement

The data used to support the findings of this study are available from the corresponding author upon request.

## Acknowledgment

The authors thank the Research Center of Medical Sciences and Pathology Department of People's Hospital of Guangxi Zhuang Autonomous Region for supporting this study.

## Funding

This study was funded by the National Natural Science Foundation of China (Grant no. 81260007) and Guangxi Natural Science Foundation (Grant no. 2017GXNSFAA198074).

## Disclosure

The authors report no conflicts of interest in this work.

## References

1. Chen Y, Chan ATC, Le Q, et al. Nasopharyngeal carcinoma. *The Lancet*. 2019;394(10192):64–80.
2. Bray F, Ferlay J, Soerjomataram I, et al. Global cancer statistics 2018: GLOBOCAN estimates of incidence and mortality worldwide for 36 cancers in 185 countries. *CA Cancer J Clin*. 2018;68(6):394–424. doi:10.3322/caac.21492
3. Chan AT, Gregoire V, Lefebvre JL, et al. Nasopharyngeal cancer: EHNS-ESMO-ESTRO Clinical Practice Guidelines for diagnosis, treatment and follow-up. *Ann Oncol*. 2012;23(Suppl 7):i83–i85. doi:10.1093/annonc/mds266
4. Chen YP, Tang LL, Yang Q, et al. Induction chemotherapy plus concurrent chemoradiotherapy in endemic nasopharyngeal carcinoma: individual patient data pooled analysis of four randomized trials. *Clin Cancer Res*. 2018;24(8):1824–1833. doi:10.1158/1078-0432.CCR-17-2656
5. McIntire JJ, Umetsu SE, Akbari O, et al. Identification of Tapr (an airway hyperreactivity regulatory locus) and the linked Tim gene family. *Nat Immunol*. 2001;2(12):1109–1116. doi:10.1038/ni739
6. Monney L, Sabatos CA, Gaglia JL, et al. Th1-specific cell surface protein Tim-3 regulates macrophage activation and severity of an autoimmune disease. *Nature*. 2002;415(6871):536–541. doi:10.1038/415536a

7. Zhu C, Anderson AC, Schubart A, et al. The Tim-3 ligand galectin-9 negatively regulates T helper type 1 immunity. *Nat Immunol*. 2005;6 (12):1245–1252. doi:10.1038/ni1271
8. Anderson AC, Anderson DE, Bregoli L, et al. Promotion of tissue inflammation by the immune receptor Tim-3 expressed on innate immune cells. *Science*. 2007;318(5853):1141–1143. doi:10.1126/science.1148536
9. Nakayama M, Akiba H, Takeda K, et al. Tim-3 mediates phagocytosis of apoptotic cells and cross-presentation. *Blood*. 2009;113 (16):3821–3830. doi:10.1182/blood-2008-10-185884
10. Ndhlovu LC, Lopez-Vergès S, Barbour JD, et al. Tim-3 marks human natural killer cell maturation and suppresses cell-mediated cytotoxicity. *Blood*. 2012;119(16):3734–3743. doi:10.1182/blood-2011-11-392951
11. Gleason MK, Lenvik TR, McCullar V, et al. Tim-3 is an inducible human natural killer cell receptor that enhances interferon gamma production in response to galectin-9. *Blood*. 2012;119 (13):3064–3072. doi:10.1182/blood-2011-06-360321
12. Anderson AC. Tim-3: an emerging target in the cancer immunotherapy landscape. *Cancer Immunol Res*. 2014;2(5):393. doi:10.1158/2326-6066.CIR-14-0039
13. Zhuang X, Zhang X, Xia X, et al. Ectopic expression of TIM-3 in lung cancers: a potential independent prognostic factor for patients with NSCLC. *Am J Clin Pathol*. 2012;137(6):978–985. doi:10.1309/AJCP9Q6OVLVSHTMY
14. Cao Y, Zhou X, Huang X, et al. Tim-3 expression in cervical cancer promotes tumor metastasis. *PLoS One*. 2013;8(1):e53834. doi:10.1371/journal.pone.0053834
15. Zhang H, Song Y, Yang H, et al. Tumor cell-intrinsic Tim-3 promotes liver cancer via NF-κB/IL-6/STAT3 axis. *Oncogene*. 2018;37 (18):2456–2468. doi:10.1038/s41388-018-0140-4
16. Wu J, Lin G, Zhu Y, et al. Low TIM-3 expression indicates poor prognosis of metastatic prostate cancer and acts as an independent predictor of castration resistant status. *Sci Rep*. 2017;7(1):8869. doi:10.1038/s41598-017-09484-8
17. Mrizak D, Martin N, Barjon C, et al. Effect of nasopharyngeal carcinoma-derived exosomes on human regulatory T cells. *J Natl Cancer Inst*. 2015;107(1):363. doi:10.1093/jnci/dju363
18. Chen TC, Chen CH, Wang CP, et al. The immunologic advantage of recurrent nasopharyngeal carcinoma from the viewpoint of Galectin-9/Tim-3-related changes in the tumour microenvironment. *Sci Rep*. 2017;7(1):10349. doi:10.1038/s41598-017-10386-y
19. Weinstein JN, Collisson EA, Mills GB, et al. The cancer genome atlas pan-cancer analysis project. *Nat Genet*. 2013;45(10):1113–1120. doi:10.1038/ng.2764
20. Chandrashekar DS, Bashel B, Balasubramanya SAH, et al. UALCAN: a portal for facilitating tumor subgroup gene expression and survival analyses. *Neoplasia*. 2017;19(8):649–658. doi:10.1016/j.neo.2017.05.002
21. Zhou LL, Ni J, Feng WT, et al. High YBX1 expression indicates poor prognosis and promotes cell migration and invasion in nasopharyngeal carcinoma. *Exp Cell Res*. 2017;361(1):126–134. doi:10.1016/j.yexcr.2017.10.009
22. Zhong YL, Jiang L, Lin H, et al. Overexpression of KIF18A promotes cell proliferation, inhibits apoptosis, and independently predicts unfavorable prognosis in lung adenocarcinoma. *IUBMB Life*. 2019;71(7):942–955. doi:10.1002/iub.v71.7
23. Liu T, Ding Y, Xie W, et al. An imageable metastatic treatment model of nasopharyngeal carcinoma. *Clin Cancer Res*. 2007;13 (13):3960–3967. doi:10.1158/1078-0432.CCR-07-0089
24. Qiang YY, Li CZ, Sun R, et al. Along with its favorable prognostic role, CLCA2 inhibits growth and metastasis of nasopharyngeal carcinoma cells via inhibition of FAK/ERK signaling. *J Exp Clin Canc Res*. 2018;37(1):34. doi:10.1186/s13046-018-0692-8
25. Roy R, Yang J, Moses MA. Matrix metalloproteinases as novel biomarkers and potential therapeutic targets in human cancer. *J Clin Oncol*. 2009;27(31):5287–5297. doi:10.1200/JCO.2009.23.5556
26. Bourboulia D, Stetler-Stevenson WG. Matrix metalloproteinases (MMPs) and tissue inhibitors of metalloproteinases (TIMPs): positive and negative regulators in tumor cell adhesion. *Semin Cancer Biol*. 2010;20(3):161–168. doi:10.1016/j.semcancer.2010.05.002
27. Thiery JP, Acloque H, Huang RY, et al. Epithelial-mesenchymal transitions in development and disease. *Cell*. 2009;139(5):871–890. doi:10.1016/j.cell.2009.11.007
28. Massague J. TGFbeta signalling in context. *Nat Rev Mol Cell Biol*. 2012;13(10):616–630. doi:10.1038/nrm3434
29. Zhou Q, Munger ME, Veenstra RG, et al. Coexpression of Tim-3 and PD-1 identifies a CD8+ T-cell exhaustion phenotype in mice with disseminated acute myelogenous leukemia. *Blood*. 2011;117 (17):4501–4510. doi:10.1182/blood-2010-10-310425
30. Sakuishi K, Apetoh L, Sullivan JM, et al. Targeting Tim-3 and PD-1 pathways to reverse T cell exhaustion and restore anti-tumor immunity. *J Exp Med*. 2010;207(10):2187–2194. doi:10.1084/jem.20100643
31. Ngiow SF, von Scheidt B, Akiba H, et al. Anti-TIM-3 antibody promotes T cell IFN-gamma-mediated antitumor immunity and suppresses established tumors. *Cancer Res*. 2011;71(10):3540–3551. doi:10.1158/0008-5472.CAN-11-0096
32. Klibi J, Niki T, Riedel A, et al. Blood diffusion and Th1-suppressive effects of galectin-9-containing exosomes released by Epstein-Barr virus-infected nasopharyngeal carcinoma cells. *Blood*. 2009;113 (9):1957–1966. doi:10.1182/blood-2008-02-142596
33. Jiang J, Jin MS, Kong F, et al. Decreased galectin-9 and increased Tim-3 expression are related to poor prognosis in gastric cancer. *PLoS One*. 2013;8(12):e81799. doi:10.1371/journal.pone.0081799
34. Yang M, Yu Q, Liu J, et al. T-cell immunoglobulin mucin-3 expression in bladder urothelial carcinoma: clinicopathologic correlations and association with survival. *J Surg Oncol*. 2015;112(4):430–435. doi:10.1002/jso.24012
35. Shan B, Man H, Liu J, et al. TIM-3 promotes the metastasis of esophageal squamous cell carcinoma by targeting epithelial-mesenchymal transition via the Akt/GSK-3beta/Snail signaling pathway. *Oncol Rep*. 2016;36(3):1551–1561. doi:10.3892/or.2016.4938
36. Sun QY, Qu CH, Liu JQ, et al. Down-regulated expression of Tim-3 promotes invasion and metastasis of colorectal cancer cells. *Neoplasma*. 2017;64(1):101. doi:10.4149/neo_2017_112
37. Hanahan D, Weinberg RA. Hallmarks of Cancer: the Next Generation. *Cell*. 2011;144(5):646–674. doi:10.1016/j.cell.2011.02.013
38. Kastan MB, Bartek J. Cell-cycle checkpoints and cancer. *Nature*. 2004;432(7015):316–323. doi:10.1038/nature03097
39. Roomi MW, Monterrey JC, Kalinovsky T, et al. Patterns of MMP-2 and MMP-9 expression in human cancer cell lines. *Oncol Rep*. 2009;21(5):1323. doi:10.3892/or_00000371
40. Li L, Li W. Epithelial–mesenchymal transition in human cancer: comprehensive reprogramming of metabolism, epigenetics, and differentiation. *Pharmacol Ther*. 2015;150:33–46. doi:10.1016/j.pharmthera.2015.01.004
41. Sundqvist A, Ten Dijke P, van Dam H, et al. Key signaling nodes in mammary gland development and cancer: smad signal integration in epithelial cell plasticity. *Breast Cancer Res*. 2012;14(1):204. doi:10.1186/bcr3066
42. Drabsch Y, Ten Dijke P. TGF-β signalling and its role in cancer progression and metastasis. *Cancer Metastasis Rev*. 2012;31 (3):553–568. doi:10.1007/s10555-012-9375-7
43. Ryu TY, Kim K, Kim SK, et al. SETDB1 regulates SMAD7 expression for breast cancer metastasis. *BMB Rep*. 2019;52(2):139–144. doi:10.5483/BMBRep.2019.52.2.235
44. Smith AL, Iwanaga R, Drasin DJ, et al. The miR-106b-25 cluster targets Smad7, activates TGF-beta signaling, and induces EMT and tumor initiating cell characteristics downstream of Six1 in human breast cancer. *Oncogene*. 2012;31(50):5162–5171. doi:10.1038/onc.2012.11

45. Lee JY, Kong G. Roles and epigenetic regulation of epithelial-mesenchymal transition and its transcription factors in cancer initiation and progression. *Cell Mol Life Sci*. 2016;73(24):4643–4660. doi:10.1007/s00018-016-2313-z

46. Zhang L, Liao Y, Tang L. MicroRNA-34 family: a potential tumor suppressor and therapeutic candidate in cancer. *J Exp Clin Cancer Res*. 2019;38(1):53. doi:10.1186/s13046-019-1059-5